

THE FORMATION OF DWARF GALAXIES IN TIDAL DEBRIS: A STUDY OF THE COMPACT GROUP ENVIRONMENT

SALLY D. HUNSBERGER AND JANE C. CHARLTON¹

Astronomy and Astrophysics Department, Pennsylvania State University, University Park, PA 16802;
 sdh@astro.psu.edu; charlton@astro.psu.edu

AND

DENNIS ZARITSKY

University of California Observatories/Lick Observatories and Board of Studies in Astronomy and Astrophysics,
 University of California, Santa Cruz, CA 95064; dennis@ucolick.org

Received 1995 October 3; accepted 1995 November 14

ABSTRACT

From *R*-band images of 42 Hickson compact groups, we present a sample of 47 candidate dwarf galaxies that are associated with the tidal tails and arms in the groups. The candidates, found in 15 tidal features, have *R* magnitudes and masses (for $M/L = 1$) in the ranges $-16.5 \leq M_R - 5 \log h_{75} \leq -11.5$ and $2 \times 10^6 M_\odot \leq M \leq 2 \times 10^8 M_\odot$, respectively. Their masses and locations are compared to the predictions of theoretical/*N*-body tidal dwarf formation scenarios. Considering the longevity of tidal debris in the compact group environment and the results of this survey, we estimate the contribution of the tidal dwarf formation mechanism to the population of dwarf galaxies observed at large in compact groups. If the majority of our dwarf galaxy candidates are confirmed as being gravitationally bound stellar systems, then a significant fraction, perhaps as much as one-half, of the dwarf population in compact groups is the product of interactions among giant parent galaxies.

Subject headings: galaxies: clusters: general — galaxies: formation — galaxies: interactions

1. INTRODUCTION

There is anecdotal observational evidence that dwarf galaxies form in the tidal debris from giant galaxy interactions. Regions of active star formation are observed at the end of tidal tails in the Superantennae (IRAS 19254–7245) (Mirabel, Lutz, & Maza 1991) and Antennae (NGC 4038/39) (Mirabel, Dottori, & Lutz 1992) systems. In Arp 105, a blue compact dwarf and an Im galaxy have formed at the ends of two tidal tails (Duc & Mirabel 1994). Finally, numerous large H I clouds are observed in the interacting pair IC 2163/NGC 2207 (Elmegreen et al. 1995), and Elmegreen, Kaufman, & Thomasson (1993, hereafter E93) suggest that some of these may form stars, detach, and become separate dwarf galaxies.

The idea that self-gravitating objects in tidal tails could evolve to become dwarf galaxies was originated by Zwicky (1956). Recent numerical simulations confirm that clumps can form within tidal tails, but the properties of the simulated dwarfs depend on the details of the modeling. The *N*-body/SPH simulations of Barnes & Hernquist (1992, hereafter BH) produce dwarf galaxies with masses in the range $1 \times 10^7 M_\odot$ to $4 \times 10^8 M_\odot$ during a single encounter between two giant galaxies. In their model, high-mass dwarfs form anywhere along the tidal tail, but small-mass dwarfs form only near the end of the tail where tidal disruption is less severe. Elmegreen et al. (1993) apply a two-dimensional *N*-body code (Thomasson 1989) to the problem of condensation of H I clouds in a tidal tail created from an extended gaseous disk, treating the gas as a dissipational particle component. They find that the velocity dispersion in the gas defines the mass of the clouds produced. Because the details of the interaction set a

“characteristic” velocity dispersion, a smaller range of dwarf galaxy masses (within a factor of 5) is produced in a single encounter. Finally, their simulations show that a large pool of gas ($\sim 10^9 M_\odot$) develops at the tip of the tidal tail from material drawn from the outer edge of the parent disk.

Hickson compact groups (HCGs) present a unique environment in which to study the tidal dwarf formation mechanism. Hickson (1982) cataloged 100 compact groups of galaxies from a systematic search of the Palomar survey prints, selecting them on the basis of population, isolation, and compactness. Radial velocity measurements (Hickson et al. 1992) and morphological studies (Mendes de Oliveira & Hickson 1994) suggest that most of the Hickson compact groups are physical associations; however, Mamon (1990) has argued that the data are consistent with many HCGs being superpositions of binary-rich loose groups, and Hernquist, Katz, & Weinberg (1995) contend that compact groups are chance projections of large filamentary structures. If the groups are real, then they have space densities comparable to the centers of galaxy clusters but velocity dispersions more like those in loose groups. This combination is conducive to the formation of tidal tails, although the tails probably last less than 1 Gyr (Barnes 1993). We utilize HCGs only as likely sites for tidal features. Our search and detection of candidate dwarf galaxies is otherwise independent of the nature and lifetime of HCGs.

From our sample of 42 Hickson compact groups, we focus on the seven groups in which we have detected tidal features and identify dwarf galaxy candidates within the tidal debris. The observational procedures and analysis are described in § 2. The properties of the dwarf candidates, i.e., the luminosity function, derived masses, and the relationship of dwarf luminosity to the distance from the parent galaxy, are compared to model predictions in § 3. In § 4 we estimate the number of dwarfs formed in tidal debris over

¹ Center for Gravitational Physics and Geometry, Pennsylvania State University.

TABLE 1
OBSERVED COMPACT
GROUPS

HCG Number		
001	028	052
003	030	054
004	031	056
005	032	057
006	033	059
007	034	089
012	037	092
013	038	094
014	040	095
016	043	096
020	046	097
024	047	098
025	049	099
026	051	100

the lifetime of a compact group and compare that number to the total number of dwarf galaxies predicted to be in this environment by the observed galaxy luminosity function.

2. DATA ACQUISITION AND ANALYSIS

We selected compact groups from the Hickson catalog (1982) on the basis of their angular size and galaxy apparent magnitudes (Hickson 1982; Hickson et al. 1992). No other criteria that might bias our search for tidal features (e.g., color, richness, or previous observations) were used. To match the angular sizes of the groups to the field of view, we selected groups with angular diameters smaller than $7'$. For redshift, we chose groups with $z \leq 0.05$ so that faint dwarfs ($M_R > -15$) would be above our detection limit. For a typical redshift, $z = 0.03$ or $cz = 9000 \text{ km s}^{-1}$, our limiting apparent magnitude of 21.5 corresponds to $M_R = -13.9$ (using $H_0 = 75 \text{ km s}^{-1} \text{ Mpc}^{-1}$, $q_0 = 0.1$). Of the 66 Hickson compact groups that satisfy these criteria, 49 were observable in November from Palomar.

We obtained Johnson *R*-band images of 42 Hickson compact groups (listed in Table 1) using the 1.5 m telescope at Palomar during 1993 November 16–20. A thinned Tektronix 2048×2048 CCD was binned by 2 in both directions and provided a 12.5×12.5 field of view with $0''.73$ pixel $^{-1}$. Two 15 minute exposures were taken of each group over the first four nights. Calibration frames (5 minute

exposures of each compact group) and standard star fields (Landolt 1992) were obtained during the last night under photometric conditions.

The data were reduced using IRAF². A median of 44 bias frames was subtracted from each image. The median of 55 images, including standard star fields, calibration frames, and offset frames (taken $10'$ from the group center), was used to flat-field images because it produced a flatter background than either twilight or dome flats. Next, we removed bad pixels and cosmic rays, combined the two 15 minute images of each group, and calibrated the images using the 5 minute photometric exposures and standard stars observed at a range of air masses.

We visually examine the images to identify the groups with interacting galaxies. About one-half of the observed groups contain interacting galaxies. The interactions are characterized by disrupted galaxies, extended luminous halos, tidal bridges, tidal arms, and/or tidal tails. We define a “tidal bridge” as an extension of material between the interacting galaxies, a “tidal arm” as an elongated or distorted spiral arm, and a “tidal tail” as a significant tail-like feature that is unassociated with a spiral arm. For the purpose of searching for tidal dwarfs, we select the seven groups that specifically exhibit tidal tails or tidal arms. Figures 1a–1d (Plates 2–5) are *R*-band images of these seven groups. Although the selection and classification of tidal features is somewhat subjective, we require that each pixel in the visually identified feature be at least 3σ above the background level. In fact, six of the groups have tidal features with pixel values 5σ above the local sky, and the true significance of any feature is much higher because it is the product of the number of pixels and the probability that each of them would be at least 3σ above background. This procedure places a lower limit on the number of tidal features in the sample, because features with surface brightnesses below $25.0 \text{ mag arcsec}^{-2}$ cannot be detected.

In Table 2, we compare our identification of tidal features to the results of a morphological study of HCGs by Mendes de Oliveira & Hickson (1994, hereafter MdOH) and sum-

² IRAF is distributed by the National Optical Astronomy Observatories, which are operated by the Association of Universities for Research in Astronomy, Inc. (AURA), under cooperative agreement with the National Science Foundation.

TABLE 2
SUMMARY OF TIDAL FEATURES

HCG Number (1)	Interacting Members (2)	Tidal Dwarfs (3)	Feature Description (4)	MdeO/H Results (5)
01	a-Sc, b-Im	3	b-tidal tail extending west, then north	a-tidal arm (I); b-tidal arm (I)
16	a-SBab, b-Sab	3	a-tidal tail extending east, undetected by MdOH	a-disturbed, IR, lopsided r.c., radio (I); b-tidal tails, peculiar r.c. (I)
26	a-Scd, b-E0	3	b-tidal tail extending NW	a-asymmetric, IR, weak radio (I); b-tail-like features, weak radio (I)
31	a-Sdm, c-Im	6	Two tidal arms extending NE from both nuclei, third tidal arm extending SE	a-disturbed, possible IR, sinusoidal r.c., WR (I,M); c-peculiar morphology, IR, peculiar r.c. (I,M)
38	b-SBd, c-Im	2	b-tidal arms north and south of nucleus	b-tidal tail, disturbed, IR (I,M); c-disturbed, possible IR (I,M)
92	c-SBa, ?	13	c-tidal tail extending SE	c-tidal arm, Seyfert, IR, radio (I,M)
92	b-Sbc, d-SB0	14	tidal tails north, undetected by MdOH; tidal arms south	b-tidal arm (I); d-tidal arm, weak radio (I,M)
96	a-Sc, c-Sa	3	a-tidal tail extending NW c-tidal tail extending east, undetected by MdOH	a-tail-like feature, Seyfert, IR, strong radio (I,M); c-extension along axis, poss. IR, radio (I)

NOTE.—Abbreviations: r.c. = rotation curve; (I) = interacting; IR = infrared; (M) = merging; WR = Wolf-Rayet spectral features.

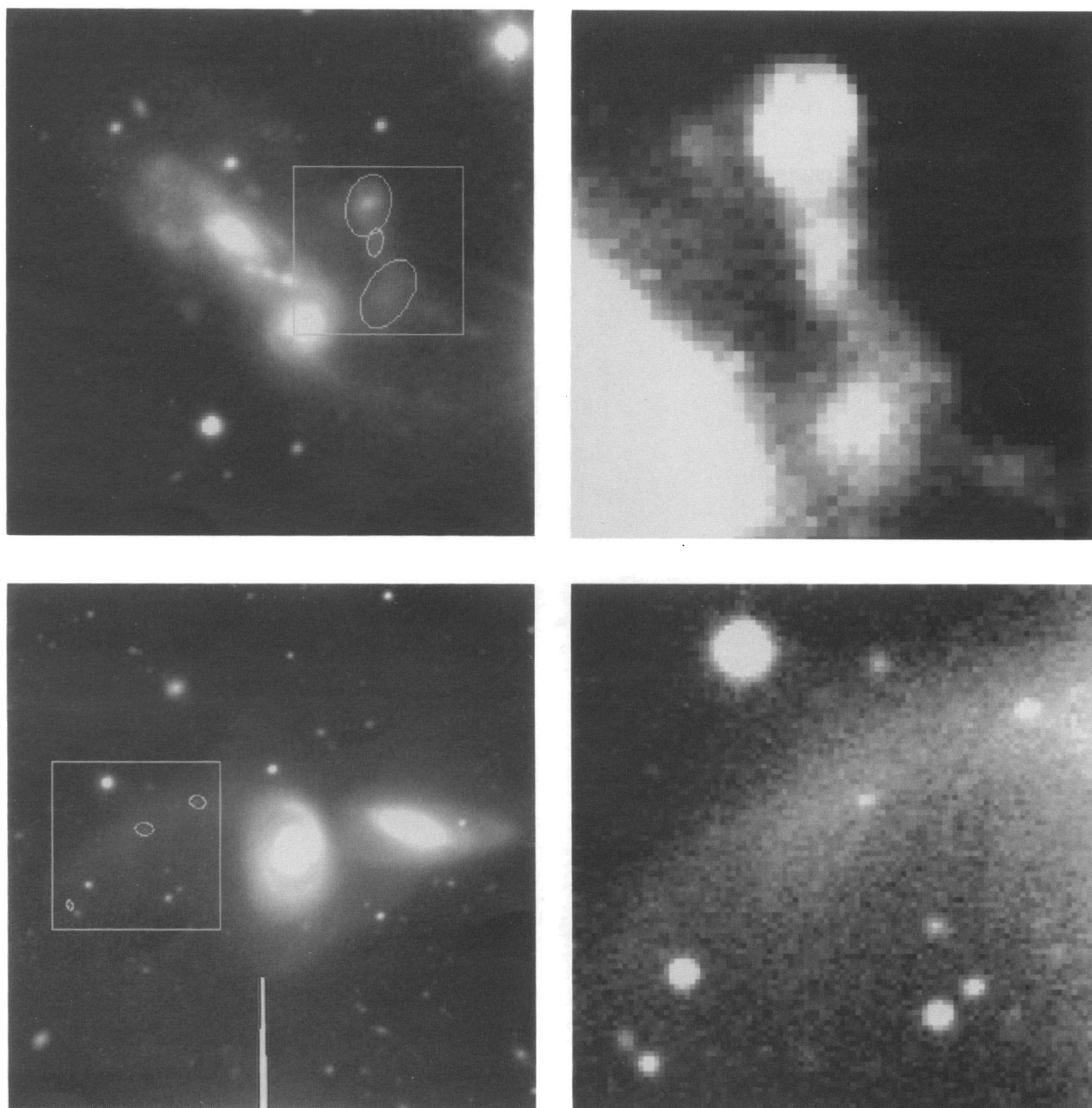
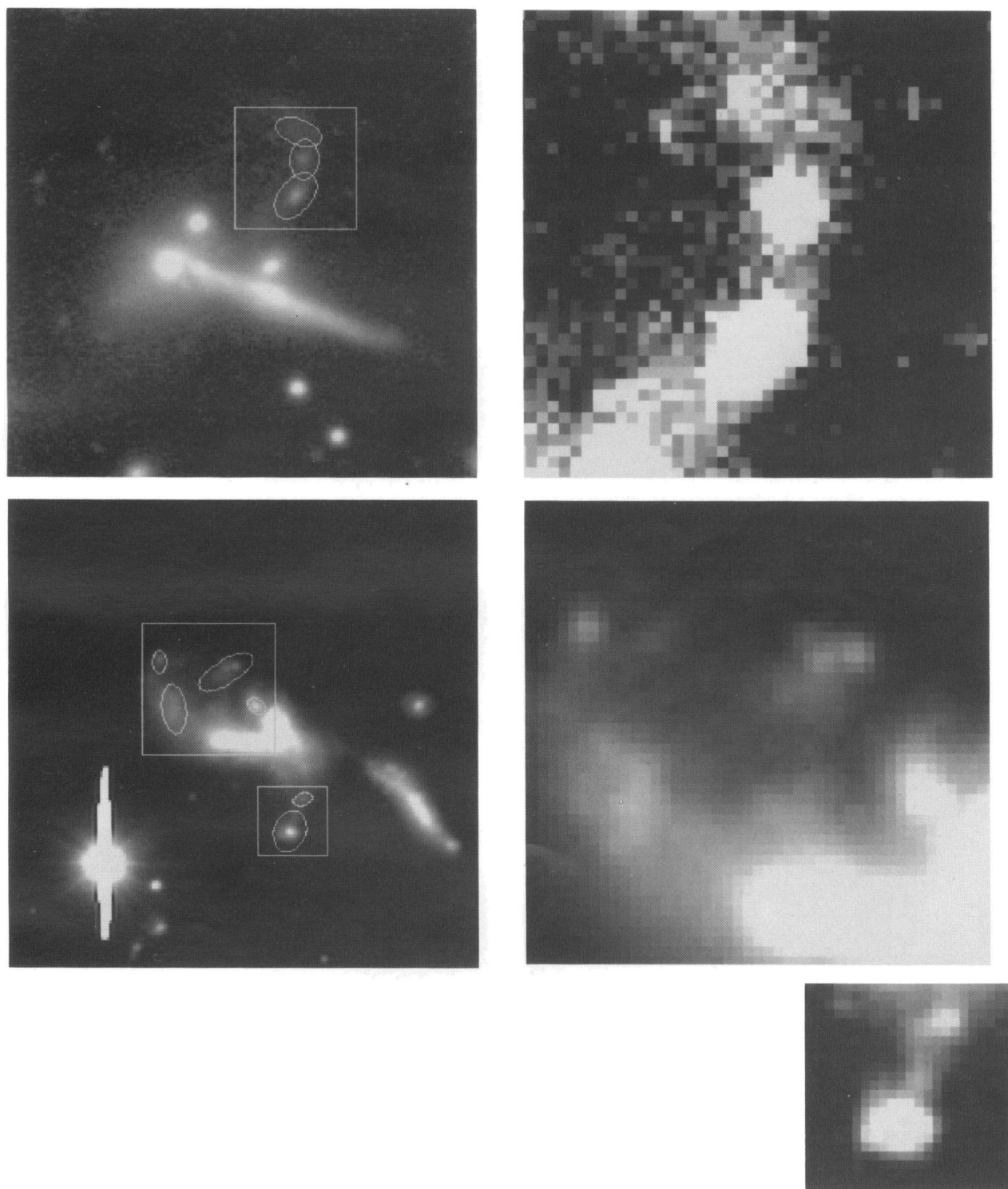


FIG. 1a

FIG. 1.—*R*-band images of interacting galaxies in our sample of Hickson compact groups. The first three panels contain full images on the left and expanded and rescaled images of the dwarf candidates on the right. The FOCAS-detected “tidal dwarf candidates” are encircled. Full frame sizes are $2' \times 2'$ for all groups except 16 and 96, which are $4' \times 4'$. (a) Images of HCG 001 (*top*) and 016 (*bottom*). (b) Images of HCG 026 (*top*) and 031 (*bottom*). (c) Images of HCG 038 (*top*) and 096 (*bottom*). (d) Images of HCG 092. At the top of the page is a group image. Member galaxy 92c appears to the left in the image and two interacting galaxies, 92b and 92d, are on the right. The width of the frame is $\sim 6'$. In the middle of the page is an enlargement of the tidal tail in 092c. At the bottom are the regions above and below the interacting pair 092bd.

HUNSBERGER, CHARLTON, & ZARITSKY (see 462, 51)

FIG. 1*b*

HUNSBERGER, CHARLTON, & ZARITSKY (see 462, 51)

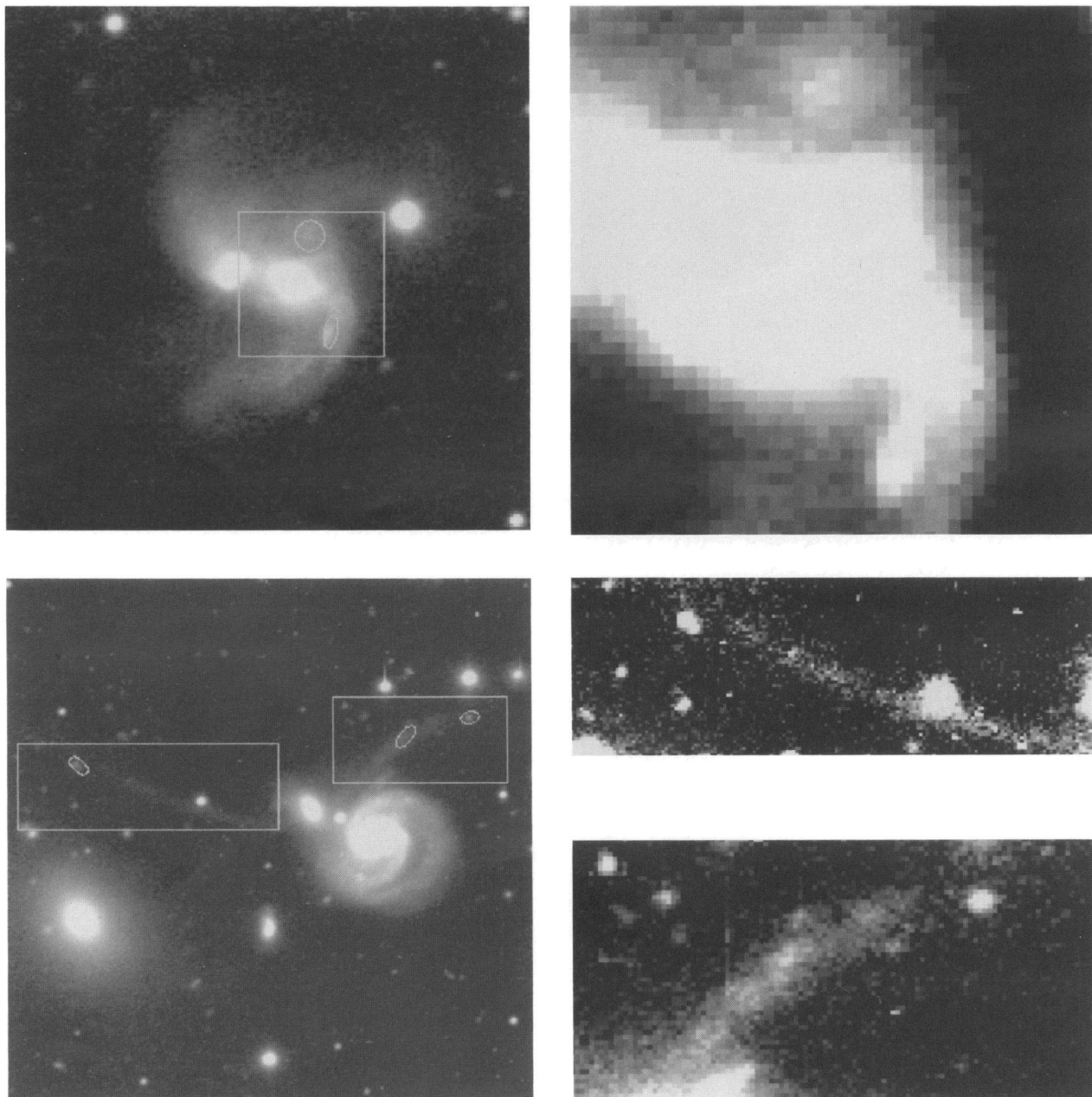


FIG. 1c

HUNSBERGER, CHARLTON, & ZARITSKY (see 462, 51)

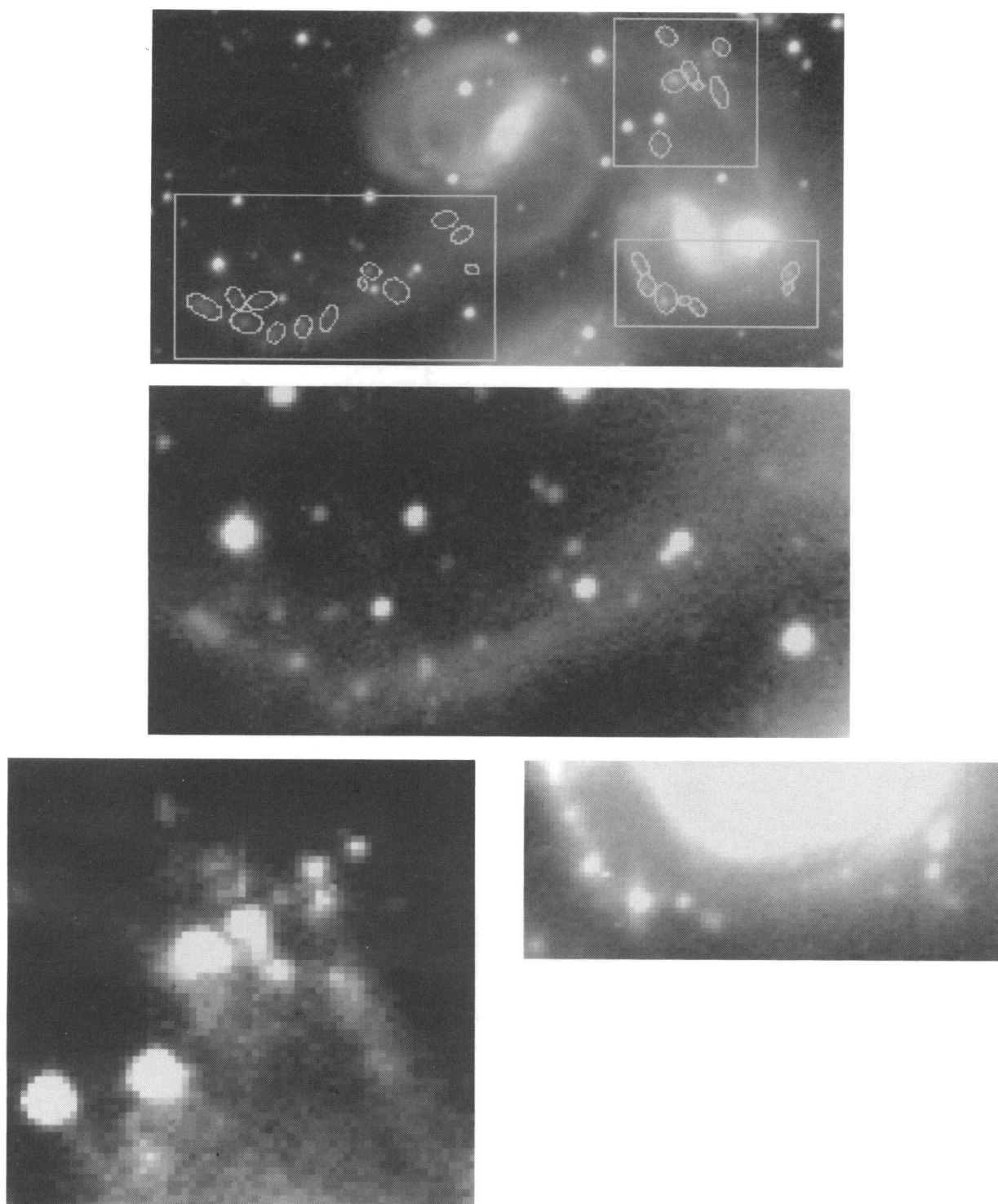


FIG. 1d

HUNSBERGER, CHARLTON, & ZARITSKY (see 462, 51)

marize the characteristics of the seven groups in our sample in which we identify tidal features. In general, we confirm the MDOH classifications. Column (1) lists the Hickson catalog group number (Hickson 1982), column (2) lists the member identification (Hickson 1982) and morphological classification (Hickson, Kindl, & Auman 1989) of the interacting galaxies, column (3) gives the number of tidal dwarf candidates for each group, column (4) describes the type of tidal feature(s) and notes with which member it is associated, and column (5) presents the results from MDOH.

We use FOCAS (Faint Object Classification and Analysis System) (Jarvis & Tyson 1981) to identify non-stellar objects in the images. The software creates a catalog of objects on the basis of user-defined detection parameters. We require that objects have at least six contiguous pixels 1.5σ above the local background. We set these values interactively to include low surface brightness dwarf candidates that are apparent by visual inspection. FOCAS computes a significance statistic for each object which we use as a detection criterion. By examining detected objects and their significance, we define our lowest acceptable significance value to be 1.0. Those objects that are classified as galaxies (i.e., extended) and that lie within a tidal feature have been designated "dwarf candidates." The 47 candidate dwarfs in the seven groups with tidal features are marked in Figures 1a–1d. From total galaxy counts provided by FOCAS, we estimate that an average of 0.7 background giants or dwarf members per group are coincident with the tidal features. Thus we expect about five of the tidal dwarfs to be unassociated with tidal features. Repeating the procedure with our star counts, we estimate that about eight stars should be coincident with the tidal debris. FOCAS actually detects five stars in the tidal features, so contamination by stars is not a major problem.

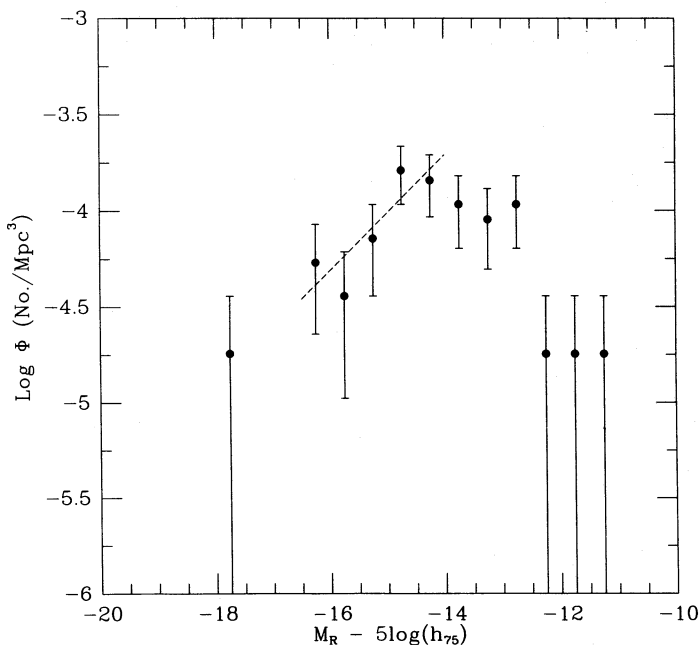


FIG. 2.—Luminosity function of tidal dwarfs. The tidal dwarf magnitudes are binned in half-magnitude intervals, and the error bars represent 1σ counting errors. The lack of objects fainter than $M_R = -14 + 5 \log h_{75}$ reflects the incompleteness of our sample at these magnitudes. Fitting to the faint end of a Schechter luminosity function, the best slope (dashed line) is $\alpha \sim -1.75 \pm 0.27$.

The magnitudes and positions of the tidal dwarfs will be the key to testing theoretical models for their formation. Because FOCAS consistently underestimates the local background within the debris, we use the IRAF POLYPHOT task to calculate the magnitudes of the dwarf candidates. Our standard star reductions indicate that there is a slight color term between the Landolt (1992) system and our observations. If the group tidal dwarfs are similar in color to the clumps in the Superantennae [(V – R) = 0.6; Mirabel et al. 1991], our color term error is only 0.024 mag. There is no color information available for our dwarf candidates, so we omit this apparently insignificant correction. Our standard star calibration uncertainties are ~ 0.02 mag. The largest uncertainties come from the determination of the local background of surrounding debris, which we estimate to be typically ~ 0.6 mag by examining the statistics (mean and standard deviation) of the local background near the object's outermost significant isophote. The dwarf candidates have absolute magnitudes $-17.7 \leq M_R - 5 \log h_{75} \leq -11.4$ with a median magnitude of $-14.2 + 5 \log h_{75}$ (where $h_{75} = H_0/75 \text{ km s}^{-1} \text{ Mpc}^{-1}$ and $q_0 = 0.1$). The corresponding luminosity function is given in Figure 2. Because there are 47 tidal dwarfs in the 42 compact groups in our sample, our estimate for the volume density of compact group tidal dwarfs is $1.8 \times 10^{-5} h_{75}^3 \text{ Mpc}^{-3}$ (using $1.6 \times 10^{-5} h_{75}^3 \text{ Mpc}^{-3}$ for the volume density of compact groups from Mendes de Oliveira & Hickson 1991). This estimate is used to normalize our luminosity function.

3. PROPERTIES OF TIDAL DWARF CANDIDATES

We fitted a line to the tidal dwarf luminosity function (shown in Fig. 2) in the magnitude range defined by the bright end of dwarf galaxies ($M_R = -16.5$) and our conservative estimate of the magnitude at which we are complete ($M_R = -14.0$). The slope of the best fit is consistent with the faint end of a Schechter (1976) luminosity function with $\alpha \sim -1.75 \pm 0.27$, which is considerably steeper than that reported by Ribeiro, de Carvalho, & Zepf (1994) for the luminosity function of compact groups, -0.82 ± 0.15 . Marzke, Huchra, & Geller (1994) detect a similar excess of faint galaxies with respect to the bright end of the field galaxy luminosity function in the CfA Redshift Survey.

Despite the reasonable agreement between our measurement of the faint end luminosity function and other previous results, we stress that our luminosity estimates, and in particular our luminosity function, are quite uncertain. First, some of the dwarf candidates may not be physically bound systems or even in the compact group. Second, there are large uncertainties in the local sky background subtraction. Third, our R-band images include H α line emission, and because these dwarfs may be actively forming stars, their luminosities may be contaminated by emission from ionized gas. However, at the typical distances of compact groups, $z = 0.03$, even a bright H II region will not be mistaken for a dwarf galaxy because its H α flux, $R \sim 24.4$, is well below the detection limit, $R \sim 21.5$. Despite the caveats mentioned above, we estimate the masses of these dwarf candidates, adopting a mass-to-light ratio of unity (consistent with the prediction of the BH model). The resulting histogram of dwarf masses is shown in Figure 3a. There is one exceptionally bright "dwarf" with an estimated mass of $6.37 \times 10^8 M_\odot$, which interestingly appears at the end of the tidal tail in HCG 001. The other tidal dwarfs have masses in the range $1.9 \times 10^6 M_\odot \leq M \leq 1.8$

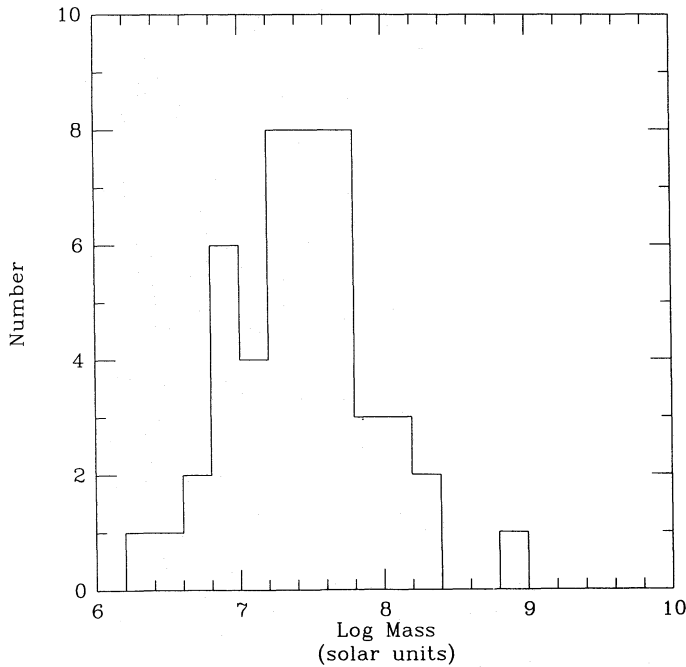


FIG. 3a

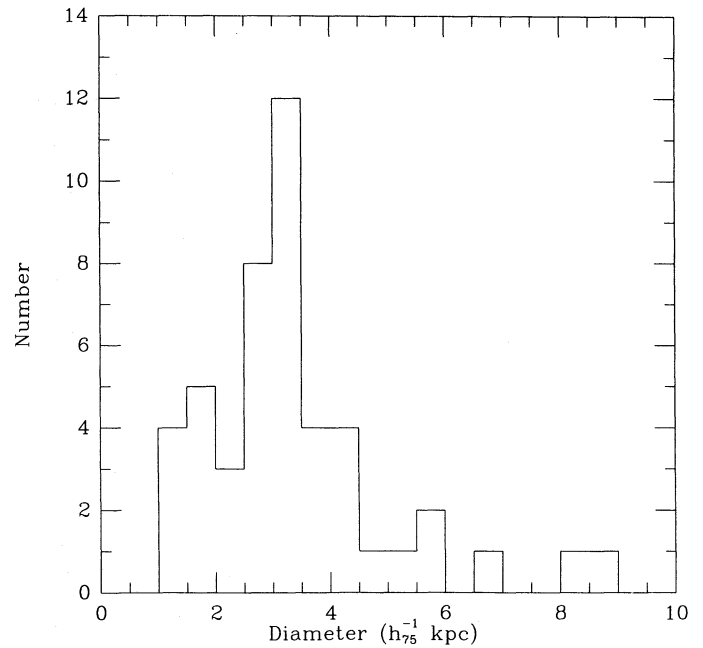


FIG. 3b

FIG. 3.—(a) Mass distribution of tidal dwarfs. This distribution is based solely on luminosity and assumes $M/L = 1$. The median dwarf mass is $\sim 10^{7.4} M_{\odot}$. (b) size distribution of tidal dwarfs. This distribution is based on circularizing the projected area of objects detected by FOCAS. The median dwarf diameter is $\sim 3h_{75}^{-1}$ kpc.

$\times 10^8 M_{\odot}$ with a median value of $2.5 \times 10^7 M_{\odot}$. Diameters are estimated from the projected areas calculated by FOCAS (see Fig. 3b). Our smallest candidate has an area of $\sim 13.5 \text{ arcsec}^2$, so the candidates are well resolved. Most diameters are between 1 and $6h_{75}^{-1}$ kpc with the median value $\sim 3h_{75}^{-1}$ kpc. Table 3 summarizes the tidal dwarf data. Column (1) identifies individual tidal features, column (2) gives the distance of each tidal dwarf from the nucleus of the parent galaxy, and columns (3), (4), and (5) list magnitude, estimated mass, and diameter, respectively.

We now discuss the spatial and mass distribution of the dwarf candidates to provide general constraints on models of tidal dwarf formation. Two recent models, by BH and E93, provide a preliminary examination of the problem. While both models produce dwarf galaxies in tidal tails with the range of masses observed both in this study and those of isolated interacting galaxies (see, e.g., Mirabel et al. 1991, 1992; Elmegreen et al. 1995), there is a basic difference in the mechanism through which the dwarfs form. In the BH model, stars in regions along the tail become gravitationally bound, and the gas later falls into those potential wells. In the E93 model, regions of gas along the tail become Jeans unstable and collapse. Are the global characteristics of our candidates consistent with either model?

The magnitude distribution in each system is shown in Figure 4. Each row of points represents candidate tidal dwarfs belonging to a particular parent galaxy. In some cases (31a, 38b, 92b, and 92d) two tidal features are combined because they are associated with the same parent. Comparisons between systems are difficult with the current data because there are fewer than four tidal dwarfs in most systems, and there are differences in the limiting magnitude between systems. We note two situations that may be indicative of a “preferred” magnitude range within a given

system. First, there is a lack of objects with magnitudes brighter than $M_R - 5 \log h_{75} = -13$ in system 16a. Second, we expect similar limiting magnitudes for systems 92b and 92c, yet the faintest candidates have $M_R - 5 \log$

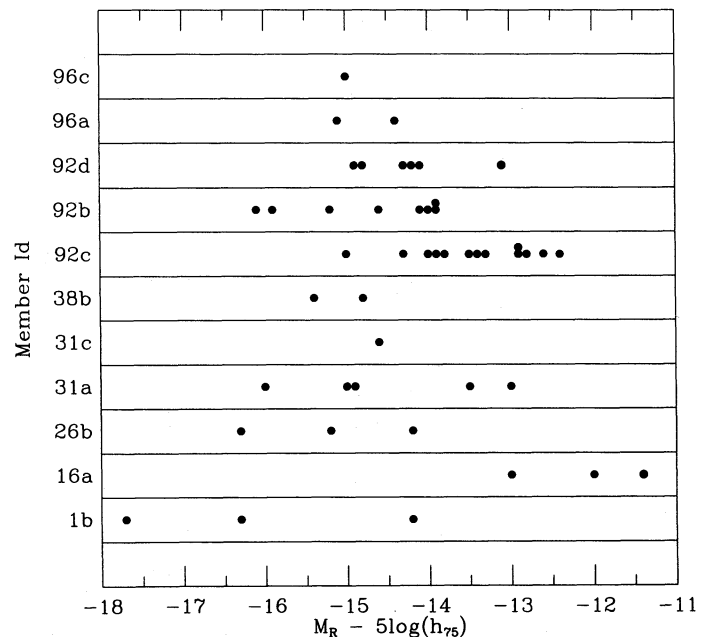


FIG. 4.—Magnitude distribution per parent galaxy. The range of magnitudes for each parent galaxy is illustrated here. Is there a preferred magnitude range for each system or is the distribution of magnitudes completely random? The results are inconclusive because most systems have too few data points to perform a valid statistical analysis. Qualitatively, we do note a lack of bright objects in system 16a and a lack of faint objects in system 92b.

TABLE 3
TIDAL DWARF SUMMARY

Name (1)	Distance (h_{75}^{-1} kpc) (2)	Magnitude ($M_R - 5 \log h_{75}$) (3)	Mass [$\log (M/M_\odot)$] (4)	Diameter (h_{75}^{-1} kpc) (5)
01b	13.66	-16.3	8.2	8.98
	16.72	-14.2	7.4	3.33
	20.82	-17.7*	8.8	8.26
16a	12.40	-13.0	6.9	1.89
	17.28	-12.0	6.5	2.00
	26.62	-11.4	6.3	1.14
26b	22.71	-16.3	8.2	6.72
	27.03	-15.2	7.8	5.57
	29.36	-14.2	7.4	5.75
31a N	5.25	-15.0	7.7	2.72
	7.16	-14.9	7.7	2.46
	9.22	-13.5	7.1	1.31
31c N	2.15	-14.6	7.6	1.26
31a S	5.04	-13.0	6.9	1.18
	6.94	-16.0*	8.1	2.59
38b N	6.29	-14.8	7.6	4.15
38b S	8.10	-15.4	7.9	2.99
92c	16.10	-12.8	6.8	3.32
	16.97	-12.9	6.9	3.00
	20.78	-12.4	6.7	2.01
	28.82	-13.4	7.1	3.89
	28.93	-13.8	7.2	2.85
	31.11	-12.6	6.8	1.83
	38.08	-13.3	7.0	3.26
	41.60	-14.0	7.3	3.15
	44.09	-13.5	7.1	3.61
	45.33	-13.9	7.3	3.00
	47.08	-12.9	6.9	3.16
	47.81	-14.3	7.4	4.13
	51.57	-15.0*	7.7	4.21
92b S	9.18	-14.6	7.6	2.81
	9.89	-14.0	7.3	1.95
	10.12	-15.2	7.8	3.04
	10.30	-15.9	8.1	3.97
	10.81	-13.9	7.3	2.63
92b N	13.25	-13.9	7.3	3.48
	21.64	-16.1	8.2	3.74
	26.52	-14.1	7.4	2.84
92d S	7.47	-14.9	7.7	2.92
	8.93	-14.1	7.4	1.92
92d N	21.03	-14.2	7.4	3.49
	22.83	-13.1	7.0	1.74
	24.97	-14.8	7.6	3.10
	31.14	-14.3	7.4	3.08
96c E	62.15	-15.0*	7.7	4.72
96a W	27.39	-14.4	7.5	5.09
	39.71	-15.1*	7.8	4.41

NOTE.—An asterisk following the magnitude indicates a bright dwarf candidate located at the end of a tidal tail.

$h_{75} = -13.9$ and -12.4 , respectively. A “preferred” magnitude range that varied among interactions, if confirmed with further observations, would support the E93 model of tidal dwarf formation.

We now examine the distribution of dwarf masses along tidal features, beginning with the richest system, HCG 92c, to search for a correlation between magnitude and distance (see Fig. 5). The data show a tendency for the dwarf luminosity to increase with distance from the parent. A Spearman rank correlation test gives a 99.3% probability that the distribution of magnitudes is not random. However, the HCG 92c tidal feature is exceptional in terms of size and richness. Because there is no apparent nearby perturber of HCG 92c, it is possible that the interacting nuclei have already merged. This tail may then be long lived, which is thought to be atypical for the compact group environment.

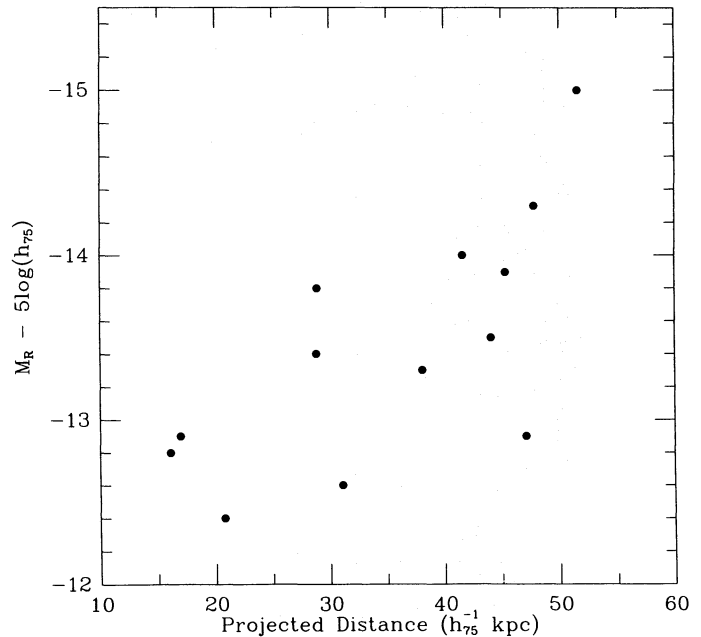


FIG. 5.—Magnitude vs. projected distance from parent nucleus (92c). With 99% confidence, there exists a linear correlation between magnitude and distance, i.e., the brightest dwarfs occur in the outer region of the tidal tail.

These data contradict the expectation that because only high-mass objects survive the large tidal forces near the center of the parent galaxy (as seen in the BH simulations) there should be a lack of faint objects in the inner region of the tail. In fact, the brightest object in each tail/arm is located at the tip in five of the 15 tidal features. This situation is analogous to that of the Antennae (Mirabel et al. 1992) and Superantennae (Mirabel et al. 1991). The presence of the brightest dwarf in the system at the end of the tidal feature is not predicted by the BH model, but can be accounted for by the E93 model if the parent has an extended gaseous disk. Clearly tidal disruption must play a role, although the inclusion of an extended gaseous disk in the parent galaxies appears to be most important.

Although both results cited above favor the E93 model, a definitive resolution of the tidal dwarf formation mechanism awaits detailed observations of the dwarfs themselves. Observations of their current star formation rates, their stellar populations, their metallicities, and the distribution of gas within them and within the tidal features are necessary.

4. DWARF FORMATION IN A DENSE ENVIRONMENT

We now estimate the fraction of all compact group dwarfs formed in tidal debris by dividing the number of dwarfs we expect to have formed in tails by the total number of dwarfs in compact groups. The number of dwarfs in each group is determined by extrapolating the luminosity function of compact groups, which is measured to have a faint end slope of $\alpha \sim -0.82$ for a sample complete to $M_B = -15.1 + 5 \log h_{75}$ (Ribeiro et al. 1994). There is some controversy regarding the slope of the compact group luminosity function because it is much flatter than that observed in clusters (Sandage, Binggeli, & Tammann 1985; Ferguson & Sandage 1991). If our adopted slope, -0.82 , is too flat, we will underestimate the number of group dwarfs and overestimate the contribution of tidal dwarfs to the general

population. We convert our R magnitudes to B by assuming a typical color for the tidal dwarfs of $B - R = 1.4$, the median value for clumps in the Superantennae (Mirabel et al. 1991). The magnitude interval of interest then corresponds to $-16.6 < M_B - 5 \log h_{75} \leq -11.6$. By integrating the extrapolated luminosity function over this magnitude range, we calculate a volume density of dwarf galaxies of $1.2 \times 10^{-4} h_{75}^3$ galaxies Mpc^{-3} . Dividing by the volume density of compact groups, $1.6 \times 10^{-5} h_{75}^3$ groups Mpc^{-3} (Mendes de Oliveira & Hickson 1991), we obtain an estimate of ~ 7.5 dwarfs per group in our magnitude interval for $h_{75} = 1$.

The number of tidal dwarfs currently being produced in tidal tails in compact groups is estimated from our data. To convert the number of tidal dwarfs seen today to the total number of tidal dwarfs formed in compact groups, we need to know the number of dwarfs formed in the past that are currently not seen in tidal features either because the tidal features and dwarfs have dispersed or because the dwarfs have merged with or been tidally disrupted by the parent galaxy. First, we estimate the average number of interactions among parent galaxies over the lifetime of a group. Let τ_g be the lifetime of a compact group and τ_t the lifetime of a tidal tail in this environment. If f_t is the observed fraction of groups with tidal features, then the number of interactions, i , that produce tidal tails over τ_g , can be expressed as $i = (\tau_g/\tau_t) \times f_t$.

The ratio of timescales τ_t/τ_g for compact groups is uncertain but can be estimated from simulations. In the merger of an isolated pair of galaxies (Barnes 1993), one can easily follow the development of tidal tails and unmistakable tidal features that exist for a significant part of the merger process. In a multiple merger (Barnes 1993), the resultant tidal debris is quickly scattered around the interacting galaxies. Tidal tails do sometimes form in a multigalaxy environment when the interaction involves only two group members, but these tails are short lived (less than one-tenth of the merger time) because they are disrupted by other galaxies. It is also difficult to distinguish such tidal features amidst the general debris from several simultaneous interactions. From these simulations, we estimate that $(\tau_t/\tau_g) \sim 0.10$. The number of interactions per group that produce tidal tails during its lifetime is then $i = (\tau_g/\tau_t) \times f_t = (1/0.1) \times (7/42) = 1.7$. Within the eight observed interactions (HCG 092 has two interactions) there are 40 tidal dwarf candidates in the magnitude interval $-18 < M_R - 5 \log h_{75} \leq -13$. This yields a production rate of 5.0 dwarfs per interaction.

The survival rate of tidal dwarfs must also be considered. E93 predict that the ultimate fate of any dwarf is linked to the mass ratio of the interacting galaxies. If the perturber mass is greater than the parent mass, the clumps in the tail will be ejected into the group at large or become satellites of the new galaxy. In the E93 simulations, tidal tails are produced regardless of the mass ratio, so we expect that the perturber mass is greater than the parent mass approximately half of the time and assume that half of the tidal dwarfs currently observed in the tidal tails will survive.

The estimated number of tidal dwarfs produced per group is (interactions per group) \times (dwarfs per interaction) \times (survival rate) $= 1.7 \times 5.0 \times 0.5 = 4.2$. This is 56% of the expected number of dwarfs throughout an entire group (7.5 dwarfs per group). Because half of the tidal dwarfs identified are in HCG 092, the estimate of the frac-

tion of tidal dwarfs is considerably lower ($\sim 30\%$) if this group is excluded from the analysis. A steeper compact group luminosity function or contamination of tidal dwarf candidates by background galaxies, foreground stars, and group dwarfs would also decrease the estimated tidal dwarf fraction. On the other hand, if some of the systems in our sample are not compact groups, then the fraction of tidal dwarfs will be underestimated because the number of interactions per real group would increase. Last, our estimate is conservative because our sample is probably not complete to $M_R = -13 + 5 \log h_{75}$. Despite the large uncertainties, we conclude that the tidal dwarf formation mechanism is a significant contributor to the dwarf population of compact groups.

5. SUMMARY

We conduct a systematic survey of tidal debris in the environment of Hickson compact groups of galaxies to address the question of whether a significant fraction of dwarf galaxies in dense environments form as a result of galaxy-galaxy interactions. In R -band images of 42 compact groups, we identify seven groups with tidal arms or tails. Within the tidal features, we find an average of 3.1 dwarf galaxy candidates (as few as one and as many as 13) per feature with magnitudes in the range $-17.7 \leq M_R - 5 \log h_{75} \leq -11.4$ and a median magnitude of $M_R = -14.2 + 5 \log h_{75}$. The resultant luminosity function for tidal dwarfs can be fitted by a Schechter function with a faint end slope of $\alpha \sim -1.75 \pm 0.27$. This is much steeper than the reported compact group luminosity function (Ribeiro et al. 1994), and so tidal dwarfs may represent an excess faint population.

We find no general correlation between the mass of tidal clumps and their projected distances along the tails. However, the richest tidal tail in our sample (92c) shows a significant correlation with luminosity increasing with radius, and in five of 15 tidal features the most luminous dwarf is at the end of the tidal feature. These results support the E93 models, which produce a large gas deposit at the end of the tidal tail opposite the perturbing galaxy.

We estimate the contribution of tidal dwarf formation and suggest that a substantial fraction (at least one-third and perhaps more than one-half) of all dwarfs in compact groups are formed during galaxy-galaxy interactions. Because tidal tails are observed in all environments, this formation mechanism could have more general implications. Confirmation of the candidates as tidal dwarfs will require H α , colors, and spectroscopy to determine star formation rates, stellar populations, and if they are gravitationally bound members of the tidal feature. Our estimate of the importance of the tidal dwarf formation mechanism will also be improved by increasing the sample, by establishing the compact group luminosity function, and by conducting simulations that more reliably predict the relevant timescales and products. *We conclude that some galaxies do not form as described by the standard hierarchical models of galaxy formation and that the fraction of compact group dwarfs produced within tidal debris is not negligible.*

We would like to thank R. Ciardullo, L. Hoffman, M. Kaufman, V. Rubin, and E. Salpeter for all their helpful comments and Bob Hill and Skip Staples for their assistance at the telescope. D. Z. acknowledges financial support from the California Space Institute.

REFERENCES

- Barnes, J. E. 1993, in *Cosmic Clips: Animations from Astronomers*, ed. S. Stephens & R. Goldsmith (San Francisco: ASP)
- Barnes, J. E., & Hernquist, L. 1992, *Nature*, 360, 715
- Duc, P.-A., & Mirabel, I. F. 1994, *A&A*, 289, 83
- Elmegreen, B. G., Kaufman, M., & Thomasson, M. 1993, *ApJ*, 412, 90
- Elmegreen, D. M., Kaufman, M., Brinks, E., Elmegreen, B. G., & Sundin, M. 1995, *ApJ*, 453, 100
- Ferguson, H. C., & Sandage, A. 1991, *AJ*, 101, 765
- Hernquist, L., Katz, N. S., & Weinberg, D. H. 1995, *ApJ*, 442, 57
- Hickson, P. 1982, *ApJ*, 255, 382
- Hickson, P., Kindl, E., & Auman, J. R. 1989, *ApJS*, 70, 687
- Hickson, P., Mendes de Oliveira, C., Huchra, J. P., & Palumbo, G. G. 1992, *ApJ*, 399, 353
- Jarvis, J. F., & Tyson, J. A. 1981, *AJ*, 86, 476
- Landolt, A. U. 1992, *AJ*, 104, 340
- Mamon, G. A. 1990, in *Paired and Interacting Galaxies*, ed. J. W. Sulentic, W. C. Keel, & C. M. Telesco (Washington: NASA), 619
- Marzke, R. O., Huchra, J. P., & Geller, M. J. 1994, *ApJ*, 428, 43
- Mendes de Oliveira, C., & Hickson, P. 1991, *ApJ*, 380, 30
- . 1994, *ApJ*, 427, 684
- Mirabel, I. F., Dottori, H., & Lutz, D. 1992, *A&A*, 256, L19
- Mirabel, I. F., Lutz, D., & Maza, J. 1991, *A&A*, 243, 367
- Ribeiro, A. L. B., de Carvalho, R. R., & Zepf, S. E. 1994, *MNRAS*, 267, L13
- Sandage, A., Binggeli, B., & Tammann, G. A. 1985, *AJ*, 90, 1759
- Schechter, P. 1976, *ApJ*, 203, 297
- Thomasson, M. 1989, *Research Rep. 162*, Dept. of Radio and Space Science with Onsala Space Obs., Chalmers Univ. of Technology, Göteborg
- Zwicky, F. 1956, *Ergeb. Exakten Naturwiss.*, 29, 344